

Supporting Information

Supramolecular assembly of thermoresponsive steroidal surfactant with oppositely charged thermoresponsive block copolymer

Maria Chiara di Gregorio,^a Marta Gubitosi,^a Leana Travaglini,^a Nicolae V. Pavel,^a Aida Jover,^b Francisco Meijide,^b Josè Vazquez Tato,^b Simona Sennato^c, Karin Schillén,^d Francesco Tranchini,^a Serena De Santis,^a Giancarlo Masci^a and Luciano Galantini^{a}*

^aDepartment of Chemistry, “Sapienza” University of Rome, P.le A. Moro 5, 00185 Rome (Italy)

^bUniversidad de Santiago de Compostela, Facultad de Ciencias, Avda. Alfonso X El Sabio s/n, 27002 Lugo (Spain)

^cDepartment of Physics and CNR-IPCF UOS Roma, “Sapienza” University of Rome, P.le Aldo Moro 5, 00185 Rome (Italy)

^dDivision of Physical Chemistry, Department of Chemistry, Center for Chemistry and Chemical Engineering, Lund University SE-221 00 Lund (Sweden)



Fig. S1. Pictures of a 5.0×10^{-3} M Na-tbutPhC sample at 25 (left) and 38 °C (right).

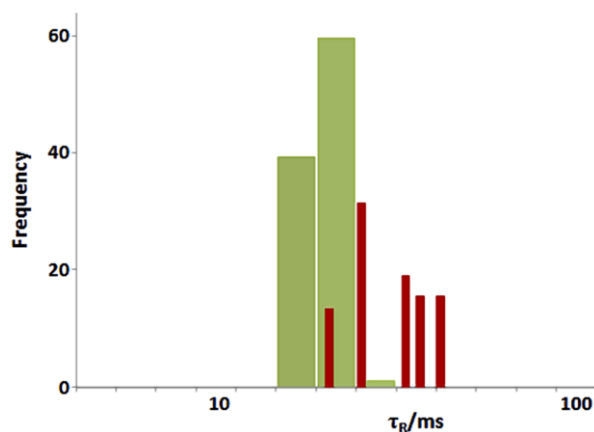


Fig. S2. Experimental intensity weighted relaxation time distribution of a solution of Na-tbutPhC with the concentration of 1.0×10^{-3} M at 36 °C obtained by DLS (green) and calculated distribution for tubules with cross section diameter of 450 nm and length of 3 μm (red).

Analysis of the DLS relaxation time distributions of Na-tbutPhC tubule dispersions (Fig. S2).

It is known that for optically isotropic rods with length L the normalized electric field correlation function may be expanded to a weighted sum of two or more exponential decays (refs 59,60 of the article).

$$g_1(q, \tau) = S_0(qL) \exp(-t/\tau_0) + S_2(qL) \exp(-t/\tau_1) + \dots + S_{2l}(qL) \exp(-t/\tau_n) \quad (1)$$

where the first term on the right-hand side is the purely translational part of the correlation function and the other exponential terms are related to the coupled rotational and translational diffusion. The scattering amplitudes $S_{2l}(qL)$ are functions of qL . We performed DLS measurements in the θ angular range of 30–90°. Considering $\theta = 30^\circ$ and a rod-length of $L = 3 \mu\text{m}$, the qL value is about 20. At this value, contributions up to the fifth term were expected to affect significantly the sum of decays. In this case, the expression of the different relaxation times of $g_1(q, \tau)$ can be written as

$$\begin{aligned} \tau_0 &= 1/Dq^2 ; \tau_1 = 1/Dq^2 + 6D_r ; \tau_2 = 1/Dq^2 + 20D_r ; \\ \tau_3 &= 1/Dq^2 + 42D_r ; \tau_4 = 1/Dq^2 + 72D_r \end{aligned} \quad (2)$$

where D and D_r are the translational and the rotational diffusion coefficient, respectively.

Using these equations at 36 °C, we estimated relaxation times of 49300, 45400, 38300, 30700, 24200 μs for tubules of a diameter $d = 450$ nm and a length $L = 3$ μm by assuming a rod-like diffusion behavior and the expressions of Broersma for D and D_r (refs 59,61,62 of the article). We also calculated the corresponding amplitudes at $qL = 20$ by using the following expression

$$S_{2l}(qL) = \frac{4l+1}{2} \frac{\left[\int_{-1}^1 P_{2l}(x) j_0\left(\frac{1}{2}qLx\right) dx \right]^2}{\int_{-1}^1 j_0^2\left(\frac{1}{2}qLx\right) dx} \quad (3)$$

where $P_{2l}(x)$ is the l th order Legendre polynomials and $j_0(z) = \sin(z)/z$.

From eq. 3, $S_0 = 0.17$, $S_2 = 0.17$, $S_4 = 0.19$, $S_6 = 0.32$ and $S_8 = 0.15$ were estimated, and from them, together with the relaxation times obtained above, a theoretical $g_1(q, \tau)$ was calculated. The calculated relaxation time distribution of this function reproduced roughly the experimental one at shorter times (Fig. S2). However, some relaxation modes expected at longer times were not revealed experimentally. Some reasons could be invoked to explain the disagreement such as the non-negligible thickness of the aggregates compared to the laser wavelength, some interparticle interactions that could take place despite the low concentration and that despite the low angle used the length of the tubules was still beyond the maximum size accessible at the q value of the measurements. It must be remarked also that the assumption of rod-like diffusion behavior of the tubules assumes that the solvent molecules are “stuck” in the interior of the tubules and just follow the tubule movements. This condition could be not rigidly fulfilled in our case due to the unusually large tubule cross section. The reformulated expressions of Broersma’s relations by Tirado et al. (ref 63 of the article) were also explored, however the result did not differ much from the one presented here.

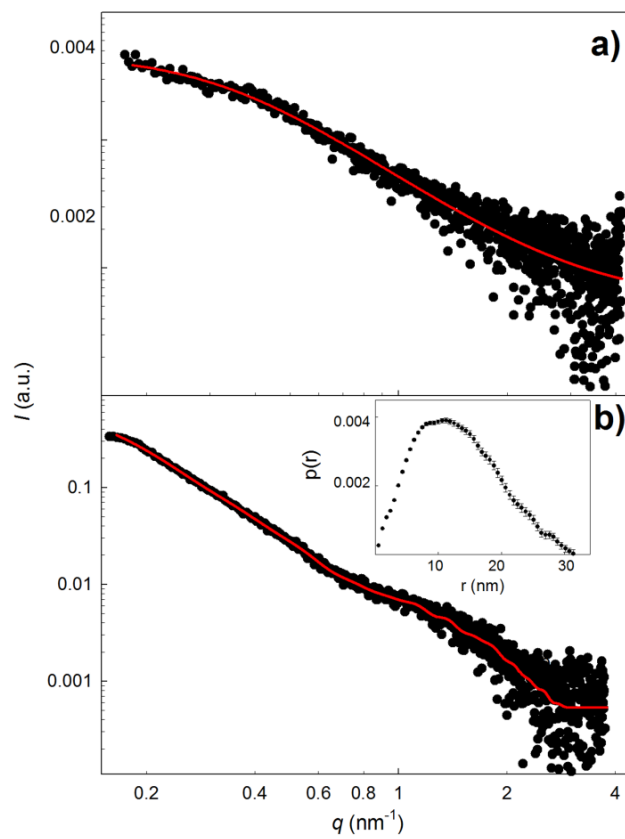


Fig. S3. Experimental (full circles) and best fitting (red lines) SAXS curves of the 1.0 wt% pNIPAAAM₁₂₀-*b*-pAMPTMA₃₀ solution at 20 (a) and 60 °C (b). The fits are based on the Gaussian chain model (a) and the IFT method (b). For the latter the pair distribution function $p(r)$ is reported in the inset.

SAXS data interpretation of pNIPAAAM₁₂₀-*b*-pAMPTMA₃₀ unimer and micelles (Fig. S3)

A SAXS curve of the pure pNIPAAAM₁₂₀-*b*-pAMPTMA₃₀ solution was collected at 20 °C in order to analyze the structure of the unimers in bulk solution at low-temperature conditions (Fig. S3a). Although clusters were expected to coexist with unimers in this conditions (see DLS results), a fit to a Gaussian chain performed by using SasView program suggested that the curve is dominated by the contribution of the unimer for which the fit provided a R_g value of 4.7 ± 0.1 nm and M_w/M_n ratio of 1.2 as a polydispersity index of the molecular weights. A lower value of 3.2 ± 0.1 nm was obtained by a Guinier plot for globular particles.

A SAXS curve of the micelles was also collected at 60 °C (Fig. S3b). An analysis of the curve using the Indirect Fourier Transform method allowed for the extraction of a $p(r)$ that was consistent with R_g and D_{max} values of 11.0 ± 0.5 and 32 ± 1 nm, respectively. It is important to remark that D_{max} in this interpretation is slightly beyond the experimental low q maximum size limit, which put some uncertainty on the reported R_g and D_{max} values. However, the latter seems not far from the DLS estimated sizes.

An aggregation number N_{agg} of 240 for the micelles was roughly estimated also as a the ratio of the extrapolated intensity at $q=0$ of the micelles, $I_{060^\circ\text{C}}$, and the unimer, $I_{020^\circ\text{C}}$, according to the equation $N_{agg}=(I_{060^\circ\text{C}}/I_{020^\circ\text{C}})$, where a negligible effect of temperature on the contrast was assumed.

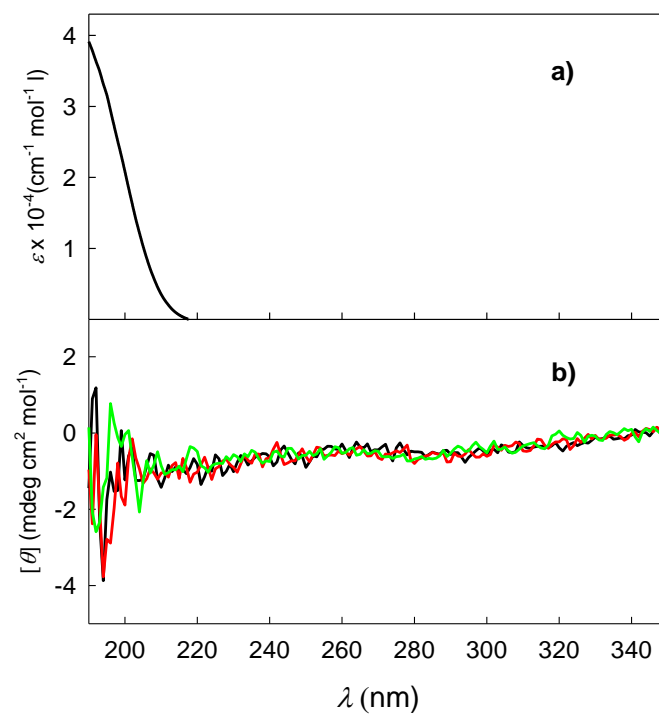


Fig. S4. UV (a) and CD (b) spectra of 1.0×10^{-3} M pNIPAAm₁₂₀-*b*-pAMPTMA₃₀ solution in carbonate/bicarbonate buffer 30.0×10^{-3} M at 25 (black), 36 (red) and 50°C (green).



Fig. S5. pNIPAAm₁₂₀-*b*-pAMPTMA₃₀/Na-tbutPhC mixture with total charge concentration of 2.0×10^{-3} M and $x^- = 0.50$ at 25 °C (left) and 35 °C after 8 hours (right).

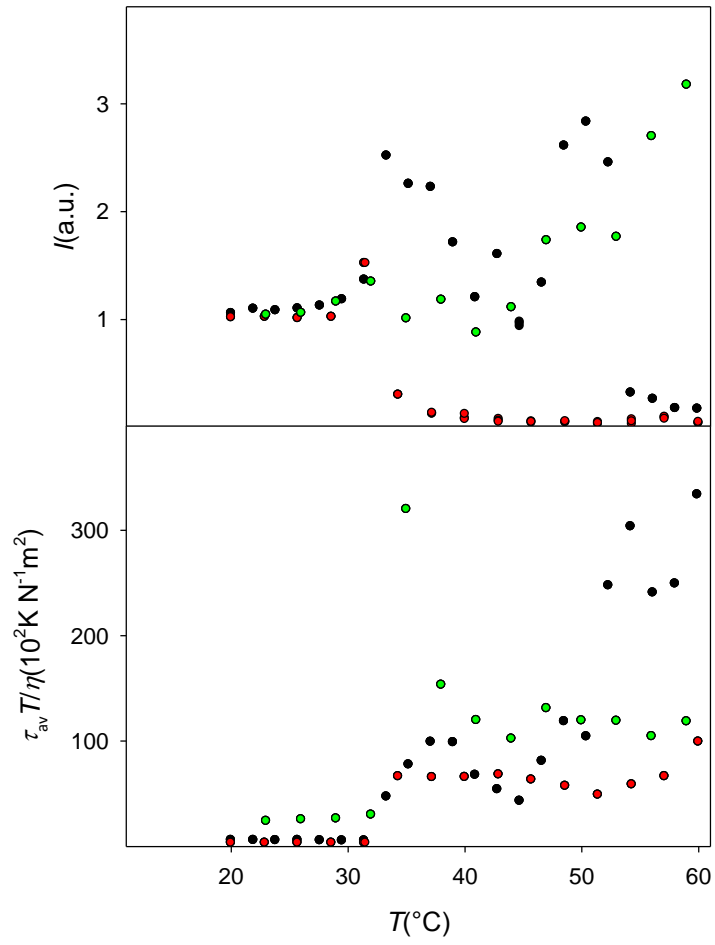


Fig. S6. Average scattered light intensity (I) and average reduced relaxation time $\tau_{av}T/\eta$ obtained from DLS measurements on mixtures at $x^- = 0.66$ (green circles), 0.50 (black circles) and 0.33 (red circles) as function of temperature.

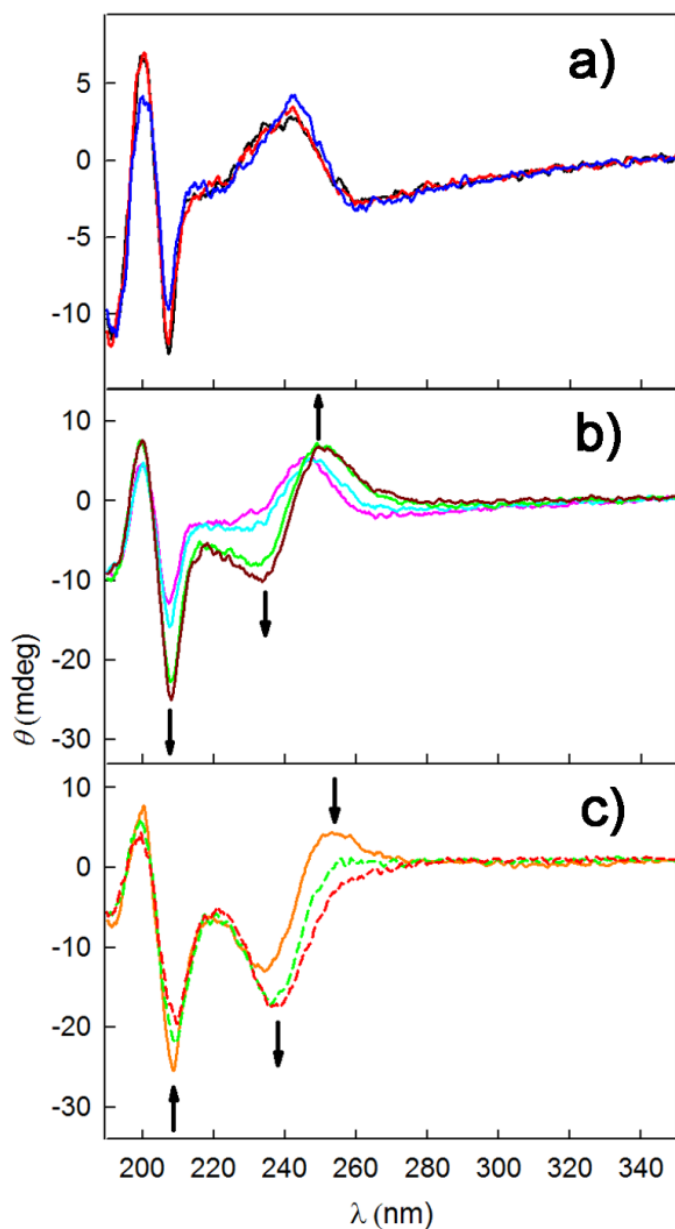


Fig. S7. CD spectra of cationic mixture with total charge concentration of 2.0×10^{-3} M and $x^- = 0.33$ at 25 (full black), 30 (full red), 32 (full blue), 34 (full pink), 36 (full cyan), 38 (full green), 40 (full brown), 50 (full orange), 60 (dashed green), 70 °C (dashed red), curves are reported in different panels a), b) and c) for clarity. Arrows indicate the evolution induced by increasing temperature.

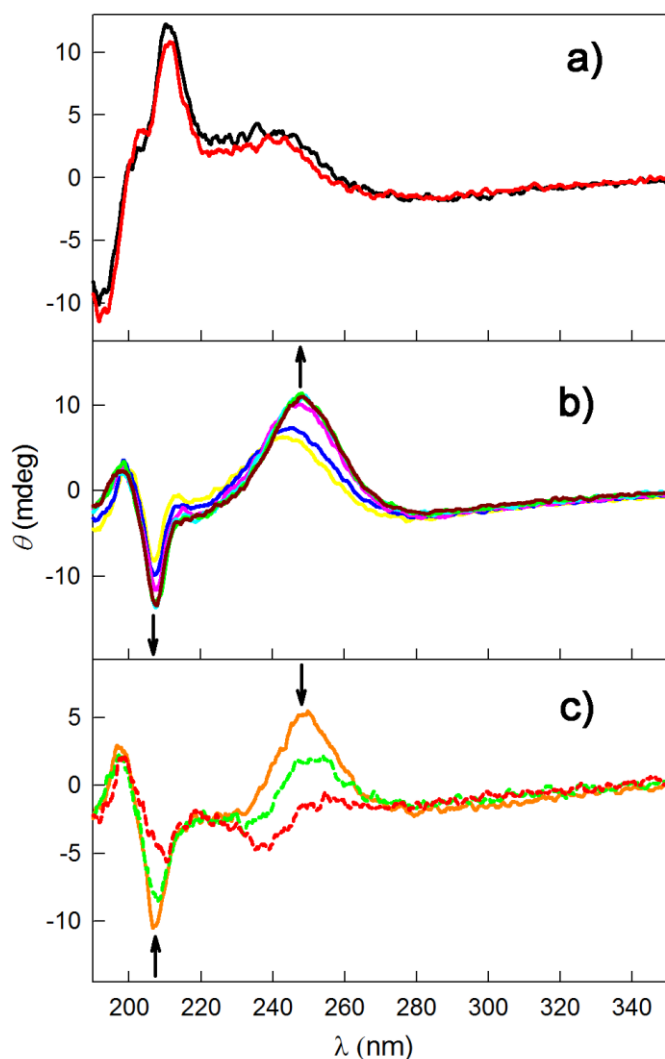


Fig. S8. CD spectra of pNIPAAm₁₂₀-*b*-pAMPTMA₃₀/Na-tbutPhC mixtures with total charge concentration of 2.0×10^{-3} M and $x^- = 0.66$ at 20 (full black), 25 (full red), 30 (full yellow), 32 (full blue), 34 (full pink), 38 (full green), 40 (full brown), 50 (full orange), 60 (dashed green) and 70 °C (dashed red), curves are reported in different panels a), b) and c) for clarity. Arrows indicate the evolution induced by increasing temperature.

Description of the CD evolutions in Figs S7 and S8.

In the presence of a larger fraction of polymer, at $x^- = 0.33$ (Fig. S7), the evolution was very similar to that of the mixture at $x^- = 0.5$ (Fig. 7), except for some very small differences. One of them was that, in this case, the first transition seemed to occur in two steps. Starting from a profile that was very similar to the one of the equimolar charge mixture, the first step occurred at 32-36 °C by a red shift of the band at 240 nm as the main variation. Only in the second step at 38°C, the transition was completed with the formation of a bisignate cotton effect. The ignition of a third stage of supramolecular rearrangement at high temperature is questionable if based on variations of the evolution trend of bands at high wavelength (220-280 nm). As a matter of fact, for temperatures > 38 °C no clear variations were observed of these bands. However, an inversion in the transformation of the minimum at 210 nm occurred at 60 °C.

On the other hand, the CD spectra of the mixtures at $x^- = 0.66$ (Fig. S8), which is richer in surfactant compared to the charge equimolar sample, were very similar to those of the pure Na-tbutPhC. A first transition occurred at 30 °C that brought to a curve almost equal to the one of the pure surfactant solution which contained the tubules. Keeping this shape the curve was slightly red-shifted by increasing temperature up to 36 °C. No variation was induced on the spectra upon further heating up to 40 °C, whereas a progressive transformation into a weak final signal was found in the temperature range 50-70 °C. Basically, the effect of polymer on the supramolecular packing of the surfactant molecules was evidently poor at this low polymer fraction. At a molecular level the arrangements of surfactant were very similar to those of the pure surfactant solution and only some variation in their stability as a function of temperature is imposed by the presence of polymer.

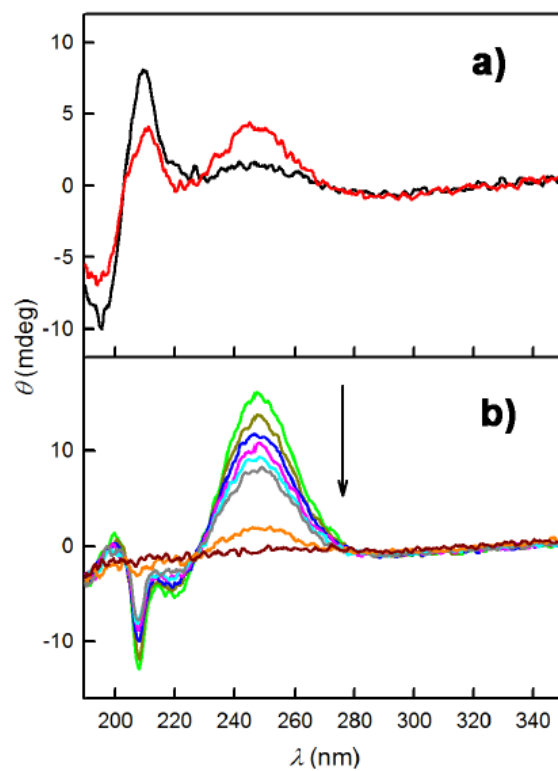


Fig. S9. CD spectra of a pNIPAAm₅₀-Na-tbutPhC based mixture at $x^- = 0.50$ are reported at temperatures of 20 (black), 25 (red), 30 (green), 32 (ocher), 34 (blue), 36 (pink), 38 (cyan), 40 (grey), 50 (orange) and 60 °C (brown); curves are reported in different panels a) and b) for clarity. Arrows indicate the evolution induced by increasing temperature.

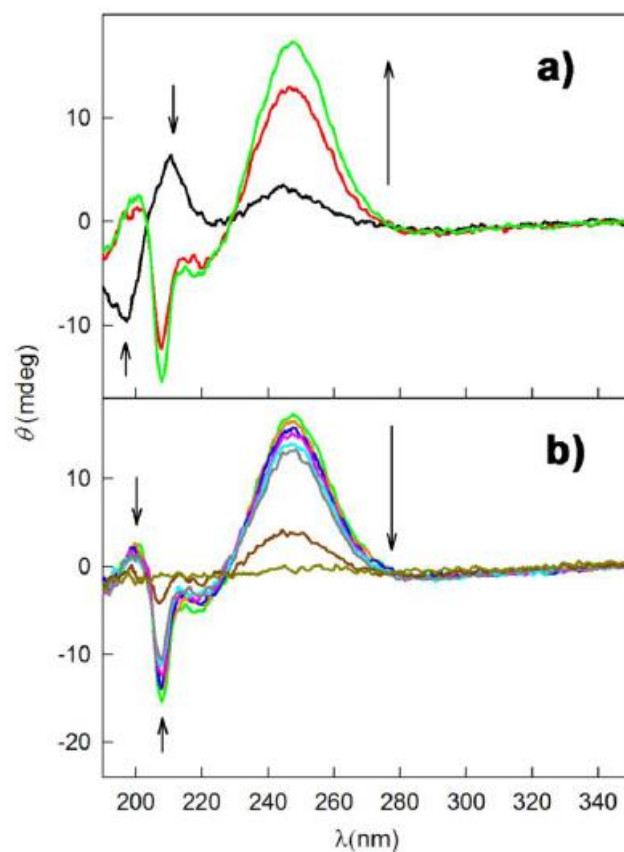


Fig. S10. CD spectra of a pNIPAAAM₉₆-b-pAMPS₃₆/Na-tbutPhC mixture at $\bar{x} = 0.50$ are reported at temperatures of 20 (black), 25 (red), 30 (green), 32 (orange), 34 (blue), 36 (pink), 40 (grey), 50 (brown), 55 (ocher); curves are reported in different panels (a) and (b) for clarity. Arrows indicate the evolution induced by increasing temperature.

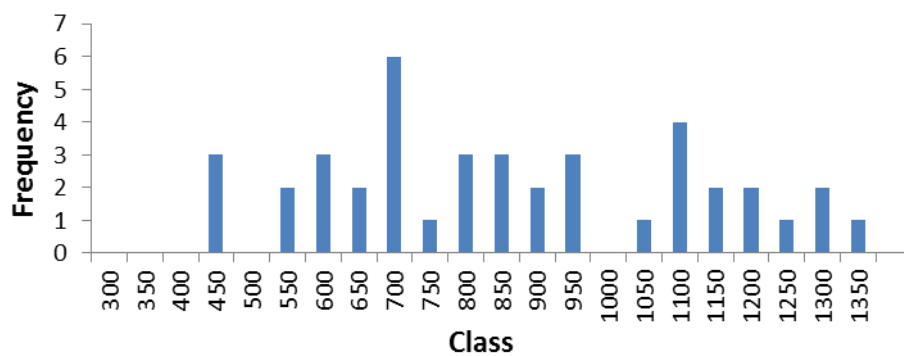


Figure S11. Length frequency histogram of the pNIPAAAM₁₂₀-b-pAMPTMA₃₀/Na-tbutPhC mixture at $\bar{x} = 0.5$ at 25 °.

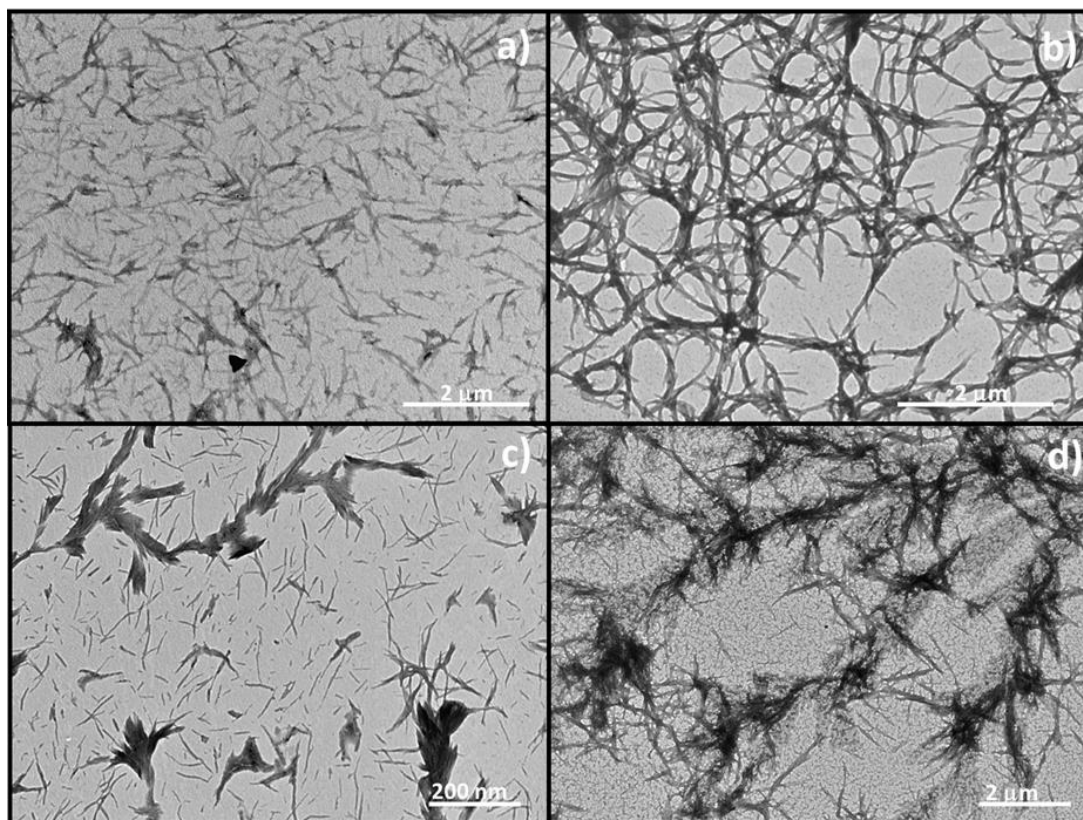


Fig. S12. TEM image of the cationic mixture at $x^- = 0.33$ (a,b) and 0.66 (c,d) at 25 °C (a,c) and 38 °C (b,d).

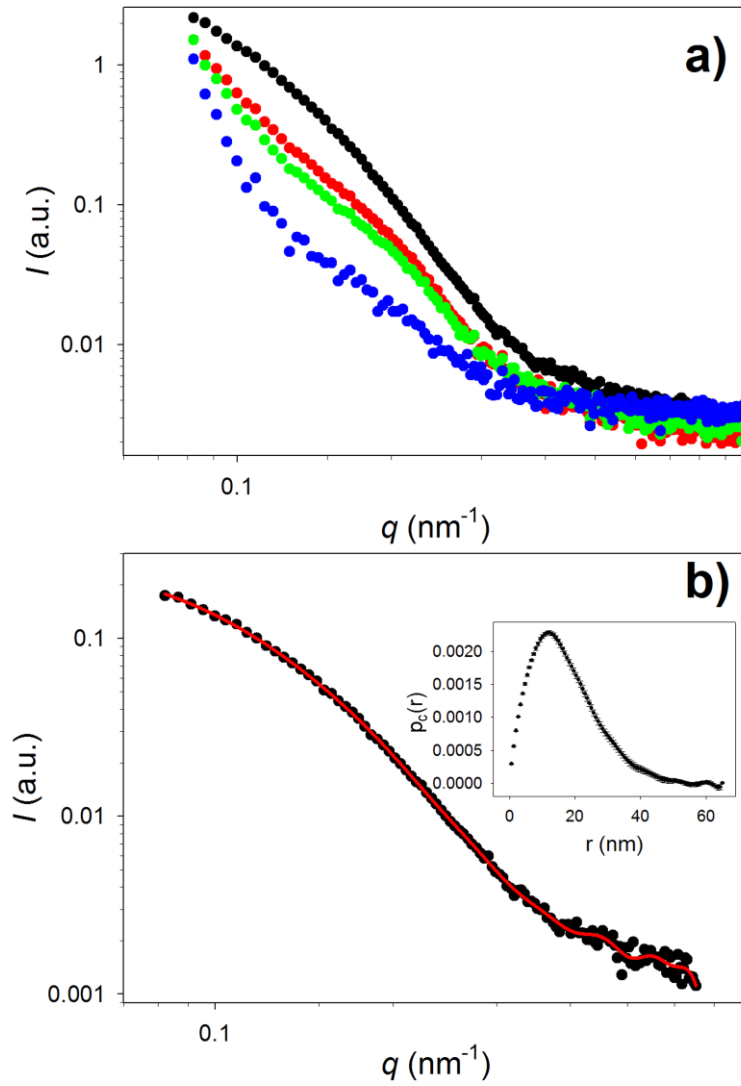


Fig. S13. a) Experimental SAXS curves of a pNIPAA₁₂₀-*b*-pAMPTMA₃₀/Na-tbutPhC mixture with $\bar{x} = 0.50$, at total charge molar concentration of 2.0×10^{-3} M and at temperatures of 20 (black circles), 40 (red circles), 50 (green circles) and 60 (blue circles) °C ; b) the best fitting IFT curve (red lines) is reported for the data at 20 °C (black circles) with the corresponding pair distribution function in the inset.